

Hippocampal gene expression profiling in spatial discrimination learning

Yolanda Robles,^a Pablo E. Vivas-Mejía,^a Humberto G. Ortiz-Zuazaga,^b Jahaira Félix,^a
Xiomara Ramos,^a and Sandra Peña de Ortiz^{a,*}

^a Department of Biology, Río Piedras Campus, University of Puerto Rico, P.O. Box 23360, San Juan, PR 00931-3360, USA

^b High Performance Computing facility, University of Puerto Rico, P.O. Box 23360, San Juan, PR 00931-3360, USA

Received 11 November 2002; revised 4 February 2003; accepted 18 February 2003

Abstract

Learning and long-term memory are thought to involve temporally defined changes in gene expression that lead to the strengthening of synaptic connections in selected brain regions. We used cDNA microarrays to study hippocampal gene expression in animals trained in a spatial discrimination-learning paradigm. Our analysis identified 19 genes that showed statistically significant changes in expression when comparing Naïve versus Trained animals. We confirmed the changes in expression for the genes encoding the nuclear protein prothymosin_α and the δ-1 opioid receptor (DOR1) by Northern blotting or in situ hybridization. In additional studies, laser-capture microdissection (LCM) allowed us to obtain enriched neuronal populations from the dentate gyrus, CA1, and CA3 subregions of the hippocampus from Naïve, Pseudotrained, and spatially Trained animals. Real-time PCR examined the spatial learning specificity of hippocampal modulation of the genes encoding protein kinase B (PKB, also known as Akt), protein kinase C_δ (PKC_δ), cell adhesion kinase_β (CAK_β, also known as Pyk2), and receptor protein tyrosine phosphatase_{ζ/β} (RPTP_{ζ/β}). These studies showed subregion specificity of spatial learning-induced changes in gene expression within the hippocampus, a feature that was particular to each gene studied. We suggest that statistically valid gene expression profiles generated with cDNA microarrays may provide important insights as to the cellular and molecular events subserving learning and memory processes in the brain.

© 2003 Elsevier Science (USA). All rights reserved.

Keywords: cDNA microarrays; Spatial discrimination learning; Laser capture microdissection; Delta opioid receptor; Protein kinase B; Receptor protein tyrosine phosphatase; Cell adhesion kinase; Protein kinase C

1. Introduction

Learning seems to have two distinct components: a short-term phase that lasts no more than several hours, and a long-term component that can last for days or longer (Alvarez, Zola-Morgan, & Squire, 1994; Kandel, Castellucci, Goelet, & Schacher, 1987; Kessner & Connor, 1972). The general view in the field is that learning and memory formation produce biochemical and structural changes at the synapse, which require alterations in gene expression and function (Albright, Kandel, & Posner, 2000; Matynia, Anagnostaras, & Silva, 2001; Tsien, 2000). Such changes in gene expression and

function are generally believed to depend on de novo RNA and protein synthesis (Castellucci, Blumenfeld, Goelet, & Kandel, 1989; Flexner, Flexner, & Stellar, 1965; Frey, Krug, Reymann, & Matthies, 1988; Montarolo et al., 1986). The most popular model suggests that phosphorylation of the cAMP Responsive Element Binding protein (CREB) is followed by induction of immediate-early transcription factors, such as Fos and ZIF268, which function as nuclear third messengers and mediate a series of downstream gene regulatory events that are mostly unknown (Bailey, Bartsch, & Kandel, 1996; Gonzalez & Montminy, 1989; Gudi, Casteel, Vinson, Boss, & Pilz, 2000; Mayr & Montminy, 2001). These downstream events probably involve the regulation of genes encoding neurotransmitter receptors, neuropeptides, protein kinases, phosphatases,

* Corresponding author. Fax: 1-787-764-3875.

E-mail address: spena@upracd.upr.clu.edu (S. Peña de Ortiz).

cytoskeletal components, and extracellular proteins related to cell–cell contact.

Recent studies have used microarray technology to assay hundreds or even thousands of genes in parallel to detect differences in expression that could be relevant to a given neurobiological state (Bonaventure et al., 2002; Geschwind, 2000; Lee, Weindruch, & Prolla, 2000b; Nisenbaum, 2002). Our aim in these studies was to apply cDNA microarrays to acquire simultaneous information of a group of genes during spatial acquisition and, in this way, obtain a better understanding of the nature of regulated genes at a specific point of the learning and consolidation process. Our approach represents a high throughput screening process that could be used to define a profile of differential gene expression as a result of a learning experience. Other studies have shown the importance of statistical analysis of gene arrays (Lee, Kuo, Whitmore, & Sklar, 2000a). Thus, we designed a statistical procedure based on Student's *t* tests for identifying differentially expressed genes. Genes showing modulated expression were selected based on the results from our statistical analysis of the replicated data and several of them were further studied by more conventional gene expression analysis approaches. Moreover, by using LCM coupled to real-time PCR we were able to confirm the spatial learning specific modulation of several of the selected candidate genes within specific hippocampal cell populations. Thus, the resulting profile can be used to select candidate genes for further studies to determine regional specificity, cellular localization, as well as specificity to spatial learning.

2. Materials and methods

2.1. Behavioral methods

2.1.1. Subjects

Male Long Evans rats weighing 270–300 g were obtained from Harlan Sprague Dawley, (Indianapolis, IN). Upon arrival rats were taken to the behavioral testing room and placed in home cages in pairs. Food and water were available at all times except when animals entered the food restriction protocol as described previously (Peña de Ortiz, Maldonado-Vlaar, & Carrasquillo, 2000; Vázquez, Vázquez, & Peña de Ortiz, 2000). Animals were kept on a 12-h on-off light/dark cycle.

2.1.2. Spatial discrimination learning

The behavioral protocols, including food restriction, habituation, and spatial training, as well as the hole-board maze used were exactly as previously described (Peña de Ortiz et al., 2000; Vázquez et al., 2000). Spatial training consisted in allowing food-restricted animals to search in the maze for food when only 4 of the 16 holes were baited. Animals were given one session a day,

consisting of five trials each, for three consecutive days. The total time to complete each trial, as well as the number of reference (visits to non-baited holes) and working (repeated visits to baited holes) errors served as the behavioral parameters used to assess spatial learning. Trained animals were sacrificed 3 h after their last trial on Day 3. All behavioral data were analyzed using one-way ANOVA. The Naïve group was subjected to the food-restriction protocol and the animals were sacrificed after reaching 85% of their starting weight without experiencing habituation or spatial training.

2.1.3. Pseudotraining

To control for changes in gene expression resulting from maze experience and not spatial learning, a pseudotrained-yoked control was used in some of the studies. Animals were food restricted and habituated as described above and this was followed by yoked-pseudotraining, which consisted of exploring and consuming food pellets in a fully baited maze (no spatial food pattern) during trials that lasted the same amount of time as the time used by the spatially Trained partner or after having consumed all the food pellets in the maze. That is, Pseudotrained animals were removed from the maze as soon as all pellets were consumed, (which in fact was also the case for spatially Trained rats, see above) or as soon as their spatially Trained partner did. In the former case, the Pseudotrained animals would spend less time in the maze than their spatially Trained partners, a situation that was more common in the initial training trials, when Trained rats spent more time finding their assigned food pellets. This was done to avoid further contextual learning after the animals had eaten all food pellets. This control served to determine the specificity of gene expression changes in the Trained rats that might be related to maze experience and not spatial discrimination learning per se. All animals were sacrificed by decapitation and their brains were removed immediately. For microarray and Northern analyses, the hippocampi were dissected, frozen on dry ice, and finally kept at -80°C until used. For in situ hybridization or LCM, whole brains were frozen and stored at -80°C until used.

2.2. Analysis of gene expression using nylon membrane cDNA microarrays

2.2.1. RNA extraction and cDNA probe synthesis

The gene profiling experiment was replicated four times. Three animals were used per condition for each replicate and hippocampi from animals in the same condition within a replicate were pooled and then used for RNA extraction. Thus, we used a total of 12 animals for each condition. In each replicate, samples from both conditions (Naïve and Trained) were treated in parallel. Total RNA was isolated from pooled tissue using

TriReagent (Sigma, St. Louis, MO) as described previously (Peña de Ortiz et al., 2000). Purified total RNA was dissolved in diethylpyrocarbonate (DEPC, Sigma) treated water and quantified in a spectrophotometer. RNA quality was assessed in a 1% agarose/formaldehyde gel, which was stained with ethidium bromide. For reverse transcription (RT), 5 μ g of total RNA from control and experimental conditions were precipitated in separate tubes and resuspended in 2 μ l of DEPC treated H₂O. Next, 1 μ l of 10 \times cDNA synthesis (CDS) Primer Mix (Atlas Array Kit; Clontech, Palo Alto, CA) was added to each sample. A master mix for 2.5 reactions was prepared containing 4.5 μ l of 5 \times Reaction Buffer, 2.4 μ l of 10 \times dNTP mix, 1.25 μ l of 100 mM dithiothreitol (DTT), 8.75 μ l ³²P α -dATP (10 μ Ci/ μ l), and 2.5 μ l Maloney Murine Leukemia Virus reverse transcriptase (100 U/ μ l) as instructed by the manufacturer. RT was carried out in a thermal cycler (Perkin–Elmer, Foster City, CA) using the following program: 70 °C (2 min), 37 °C (20 min), 42 °C (30 min), 45 °C (15 min), 50 °C (25 min), and 4 °C. The RNA and primer mix were subjected to the two initial temperature steps. Once the temperature reached 37 °C, 7 μ l of the master mix were added and the reaction was continued following the temperature program described above. At the 42 °C step, an additional 1 μ l of MMLV reverse transcriptase was added. The reaction was terminated at the end of the 50 °C step by adding 1 μ l of Termination mix. The labeled probe was purified using Nick Columns (Amersham-Pharmacia Biotech; Piscataway, NJ).

2.2.2. cDNA microarray hybridization

The cDNA complex probe was used to hybridize Atlas Rat cDNA Expression Arrays (Clontech). Membranes were prehybridized in 5 ml of ExpressHyb (Clontech) solution containing 1.5 mg/ml of heat-denatured sheared salmon sperm DNA (ssDNA; Stratagene; La Jolla, CA) for 30 min in a hybridization oven at 68 °C. The cDNA labeled probe (5 \times 10⁶ cpm, specific activity = 3–4 \times 10^{8–9}) was then incubated with 5 μ l (1 μ g/ μ l) of C₀t – 1 DNA per 200 μ l of probe at 100 °C and then placed in ice for 2 min. The probe was added to 5 ml of hybridization solution (ExpressHyb) containing 1.5 mg/ml of heat-denatured ssDNA and incubated overnight in rolling bottles at 5–7 rpm and 68 °C. Next, hybridization solutions were drained and membranes were washed four times with 2 \times standard sodium chloride/sodium citrate solution (SSC), 1% sodium dodecyl sulfate (SDS) at 12–15 rpm and 68 °C. These washes were followed by two additional washes with 0.1 \times SSC, 0.5% SDS. The wet membranes were then tightly wrapped in plastic film (to prevent drying) and exposed to a phosphorimager screen (Bio-Rad, Hercules, CA) at room temperature for 12–14 days. The screen was then scanned in a phosphorimager (Molecular Imager GS-525, Bio-Rad) at 100 μ m resolution. Each nylon

array was used once. Each replicate in the experiment included cDNA probes prepared from Trained and Naïve rats, which were processed in parallel throughout the experiment using separate nylon array membranes in the same replicate.

2.2.3. Data analysis

After phosphorimaging, the Atlas Image software 1.0 (Clontech) was used for aligning the arrays with a gene identification grid and for calculating background signal. We also developed software to normalize the expression values from several experiment repetitions. The software was developed on the Linux operating system (www.linux.org) using the python programming language (www.python.org) with the Numerical Python extension package for array arithmetic (numpy.sourceforge.net). The expression value for each gene was normalized by first subtracting the background reported by the Atlas Image software, then dividing each intensity by the mean signal of all the housekeeping genes (including GAPDH, α tubulin, cytoplasmic β actin, myosin heavy chain 1, ribosomal protein S29 40S subunit, polyubiquitin, phospholipase A2 precursor, and hypoxanthine-guanine phosphoribosyltransferase) or the mean signal of all the genes on the array. These housekeeping genes have been shown to remain relatively constant in a variety of tissues, cells, diseases and developmental stages (Adams, Kerlavage, Fields, & Venter, 1993; Liew et al., 1994). The background subtraction and normalization caused multiple genes to have negative expression values in at least one of the conditions. Rather than changing the negative values to zero, we decided to keep the negative values unchanged for our statistical analysis. We consider these normalized expression values to be directly comparable between conditions and across repetitions. The normalized expression values were transferred to the R statistical package (Ithaka & Gentleman, 1996) and a paired Student's *t* test was performed to test for statistical significance in expression levels between two conditions. The supplemental site for the paper (<http://www.hpcf.upr.edu/~humberto/cmb/microarray/spatial/>) has a copy of the programs for reading the Atlas Image report files, normalizing the expression data, and performing the statistical tests. Significance was accepted at $*p < .05$.

2.3. Molecular validation studies

2.3.1. Oligonucleotides probes

Oligonucleotide probes were based on the rat cDNA sequences reported for prothymosin _{α} , DOR1, and cadherin *K* in the GenBank database. The 40–41 bp antisense oligonucleotides were designed to contain 50–51% C content for optimal hybridization kinetics. The sequence of the prothymosin _{α} and DOR1 antisense oligonucleotides used for hybridization was: 5' CTC

GAA GGT GAC CAC GTT TAA ATT CTG AGA CGG GAA GTG G 3'; 5'CTT CAG CTT AGT GTA CCG GAC GAT TCC AAA CAT GAC GAG 3'; and 5' GGA GTC TTT GTC ACT GTC CAT CCC TCC GTA CAT ATC TGC CA 3', respectively. All oligonucleotides were synthesized and purified by HPLC at Life Technologies (Frederick, MD). For in situ hybridization, probes (100–125 ng) were labeled on their 3' end using terminal transferase (Promega; Madison, WI) and [$\alpha^{33}\text{P}$]dATP (200–250 μCi) as described previously (Peña de Ortiz et al., 2000). For Northern blot analyses, the 3' end labeling reactions were performed with 50 ng of oligonucleotide and 100 μCi of [$\alpha^{32}\text{P}$]dATP. All oligonucleotides were labeled to a specific activity of at least 1×10^8 cpm/ μg .

2.3.2. Northern blotting

Northern blot analysis was performed according to Peña de Ortiz et al. (2000). Additional Naïve and Trained animals were used. Hippocampi from three animals were pooled for each RNA extraction. The experiment was repeated three times for a total number of animals used per group of 9. The RNA samples (10–20 μg) were electrophoresed in a 1.2% agarose/formaldehyde gel and transferred to a nylon membrane (Genescreen; Boston, MA) using standard procedures. Blotted RNAs were stained with methylene blue as described (Peña de Ortiz et al., 2000) and scanned using a GS-700 densitometer (Bio-Rad) to verify homogeneous loading of RNA among the lanes. Pre-hybridization was done for 30 min at 52 °C in 5 ml of Quick Hyb solution (Stratagene) containing 300 $\mu\text{g}/\text{ml}$ of ssDNA (Stratagene). Hybridization was carried out overnight at 52 °C in 5 ml of Quick Hyb solution containing ssDNA (300 $\mu\text{g}/\text{ml}$) and 1.25×10^6 cpm/ml of labeled oligonucleotide probe. Membranes were washed according to the manufacturer's instructions and exposed to an autoradiographic film with two intensifying screens at –80 °C. Northern analysis was repeated with three different sets of animals per the Naïve and Trained groups. Densitometric data was subjected to Student's *t* test or one-way ANOVA coupled to multiple comparisons testing using the Newman–Keuls post-test, $N = 3$.

2.3.3. In situ hybridization

Fresh frozen coronal sections with a 20 μm thickness, obtained from Naïve and Trained animals ($N = 5$), were treated as described previously (Peña de Ortiz et al., 2000). End labeled antisense oligonucleotides were diluted at 10,000–40,000 cpm/ μl in hybridization solution as described (Peña de Ortiz et al., 2000). We used a probe competition control to show specificity of hybridization. The control sections were pre-incubated for 2 h at room temperature with a 100 \times excess of unlabeled antisense oligonucleotide probe. For these control sections hybridization was done in the presence of 100 \times

unlabeled oligonucleotide in addition to the labeled probe. Hybridization was done overnight at 37 °C and then the sections were washed as described. Sections were dehydrated and allowed to air dry before they were autoradiographed by exposing them to Hyperfilm βmax (Amersham-Pharmacia) with two intensifying screens at –80 °C for 3–7 days. Molecular hybridization detected on film autoradiograms was analyzed densitometrically. Films were scanned with the GS-700 densitometer (Bio-Rad) and optical density (OD) measurements were analyzed using the Multi-Analyst Software Package (Bio-Rad). Specifically, densitometric values were taken from regions of interest and from areas on the films of minimum and maximum optical densities (ODs). The in situ hybridization study was repeated three times with sections from 10 different animals per condition. Densitometric values were obtained from a set of 2–4 slides per animal. Each slide contained 3–4 sections, each of which was analyzed densitometrically and the data was then averaged. For statistical analysis of measures taken from different films, each measurement was normalized using the following formula: (measured OD – minimum OD)/(maximum OD + minimum OD). Specific differences in expression for each particular brain region were assessed using the Student's *t* test.

2.3.4. Laser capture microdissection (LCM) and RNA isolation from LCM-procured cells

Coronal fresh frozen sections (10 μm thick) containing the dorsal hippocampal formation from the brains of Naïve, Pseudotrained, or Trained rats ($N = 3$) were sectioned in a cryostat (–18 °C) and placed onto uncharged microscope slides (Fisher, Caguas, PR). The sections were stained by dipping in 0.1% Thionin for 1 s. This was followed by a wash in ultrapure H_2O for 1 s and then dehydration in a 70% (30 s), 95% (1 min), and 100% (1 min) ethanol series. Next, the sections were placed in xylene for 5 min and then allowed to dry in a fume hood for 30–60 min. Cells from different regions of hippocampus (dentate gyrus, CA1 and CA3) were microdissected by using a PixCell II Laser Capture Microscope with an infrared diode laser (Arcturus Engineering, Santa Clara, CA). In brief, the dehydrated tissue section was overlaid with a thermoplastic membrane mounted on optically transparent caps and the cells were captured by focal melting of the membrane through laser activation. The laser parameters were: 20 ms of laser pulse duration, 20 mW of laser power, and 30 μm of laser spot size. LCM was done on three slides, containing four coronal sections, from each animal. For each slide, LCM was done bilaterally on the granule and pyramidal cell layers of the hippocampus of all four sections. The same cap was used for the other slides from the same animal, until its entire surface was covered with cells. A different cap was used for cells from the dentate gyrus, CA1 or CA3 subregions. Cells

attached to the cap were immediately used for RNA isolation.

We purified RNA by using the PicoPure total RNA isolation Kit (Arcturus Engineering, Mountain View, CA) according to the instructions of the manufacturer. Briefly, the transfer film cap containing the LCM-derived cells was inserted into a 500 μ l microcentrifuge tube containing 50 μ l of Extraction Buffer. The tube was inverted, in order to ensure detachment of cells from the cap, and incubated inverted at 42 °C for 30 min in a humidified incubator. After gently vortexing the cap end of the tube, the tube was centrifuged at 10,000 rpm for 1 min to remove all fluid from the cap surface. The transfer film cap was removed and the tube containing the cell extract was placed in ice. Next, 50 μ l of extraction buffer was pipetted onto the Purification Column filter membrane, which was incubated for 5 min at room temperature. The purification column was then centrifuged at 12,000 rpm for 1 min. We then added 50 μ l of 70% ethanol to the cell extract and 100 μ l of the resulting mix was loaded onto the preconditioned purification column. The purification column was centrifuged for 1 min at 12,000 rpm, followed by addition of 50 μ l of Wash Buffer and centrifugation for 1 min at 12,000 rpm. This last step was repeated once again. All traces of wash buffer were removed by a final centrifugation of the column for another min at 14,000 rpm. Then, 20 μ l of Elution Buffer was added directly onto the column, followed by its incubation for 1 min at room temperature. After this time, the purification column was centrifuged at 12,000 rpm to elute the RNA. The quality and approximate yield of RNA was analyzed spectrophotometrically. In addition, the integrity of the mRNA samples was confirmed by performing standard RT-PCR for rat GAPDH and observing the amplification products by agarose gel electrophoresis. The sequences of the GAPDH primer set were: forward—5' TGACAA AGTGGACATTGTTGCC 3' and reverse 5' AAGATG GTGATGGGTTTCCCG 3'. The RNA sample was then stored at -80 °C until used. For the mock reactions, all steps were followed as with the standard tests, except that the reverse transcriptase was not added during the initial RT. Thus, any obtained products from PCR would originate from contaminating genomic DNA within the RNA samples.

2.3.5. SYBR green-based real-time quantitative PCR studies

For real-time PCR, cDNA was obtained from total RNA samples of hippocampal subregions using the TaqMan RT Reagents (Applied Biosystems, Foster City, CA). Briefly, 100 μ l of reaction mixture containing 250 ng of RNA, 500 μ M of each dNTP, 1 \times TaqMan RT buffer, 5.5 mM MgCl₂, 2.5 μ M random hexamers, 40 U RNase Inhibitor, and 125 U MultiScribe RT enzyme was incubated at 25 °C for 10 min followed by incubation

at 48 °C for 30 min. The reaction was stopped by incubating at 95 °C for 5 min. To generate the standard curves we also synthesized cDNA from the rat whole hippocampus. The cDNA samples were stored at -20 °C.

Specific primers for PKB, PKC δ , CAK β , and RPTP ζ/β were designed to work in the same cycling conditions as those for the primers for 18S rRNA (Ambion, Austin, TX), which was used as an internal control or reference gene. The following internet sites were used for a successful design of primers: The DNA mfold server of Dr. Michael Zuker (<http://bioinfo.math.rpi.edu/~fold/dna/form1.cgi>) was used to analyze secondary structure of the template; the primer3 program (http://www-genome.wi.mit.edu/cgi-bin/primer/primer3_www.cgi) was used to design the primers; the Operon company provides an internet site (<http://www.operon.com/oligos/toolkit.php>) that was used to analyze primer-dimer formation; and finally the specificity of the primers was verified using the Basic Local Alignment Search Tool (<http://www.ncbi.nlm.nih.gov/blast/>). Real-time PCR was performed using an iCycler iQ Real-time PCR Detection System (Bio-Rad, Hercules, CA) and the QuantiTect SYBR Green PCR kit (QIAGEN, Valencia, CA) according to the manufacturer's instructions. Briefly, 5 μ l of cDNA were combined with 200–400 nM of each primer, 1 \times QuantiTect SYBR Green PCR Master Mix (HotStarTaq DNA polymerase, quantiTect SYBR green PCR buffer, dNTP mix, SYBR green I, and ROX), MgCl₂ (when required) and PCR-grade water to a volume of 50 μ l. Primers were synthesized at Invitrogen. The sequence of each primer, and the concentrations of primer and Mg²⁺ were as follows: PKB (forward: 5'-GCCT GAGGTGCTAGAGGAC-3', reverse: 5'-TCCTCCTC TAGAAGGGCAG-3') at 200 nM each and 3.5 mM MgCl₂; PKC δ (forward: 5'-GTTTCATCGCCACCTTCT TTG-3', reverse: 5'-ATTTCTTATGGATGGCAGCG-3') at 400 nM each and 2.5 mM MgCl₂; CAK β (forward: 5'-CTGAGCCTTGCGTCCTACC-3', reverse: 5'-CAG CACATTGCAGTCCCTC-3) at 400 nM each and 2.5 mM MgCl₂; and RPTP ζ/β (forward: 5'-AATGGTGC AGCTTTGCCTG-3', reverse: 5'-CAGATAACAGAA CTGGACTC-3') at 300 nM each and 2.5 mM MgCl₂. The sizes of the amplification products were between 100 and 200 bp, which are in the optimal range to perform real-time PCR (Bustin, 2000).

The cycling conditions for all primers were the following: 95 °C for 15 min to activate the HotStarTaq polymerase, followed by 40 cycles consisting of two steps, 15 s at 95 °C (denaturation), and 30 s at 60 °C (annealing/extension). The PCR program was followed by a melting temperature program as follows: 1 min at 95 °C (denaturation) and 2 min at 55 °C (annealing), followed by 101 steps lasting 8 s each through which temperature ranged from 55 to 95 °C and each step differed from the previous by 0.4 °C. Amplification plots

depicting the results of reactions carried out with seven serial dilutions of rat hippocampal cDNA (ranging approximately from 12.5 ng to 200 pg) were produced in order to calculate the threshold cycle (C_t). To confirm amplification specificity, the PCR products from each primer pair were subjected to agarose gel electrophoresis and melting temperature analysis. For each reaction, standard curves of C_t versus the log of cDNA dilution for both target and reference genes were generated. Since all reactions were done in triplicate, the mean C_t was used for plotting. The regression coefficient for plotting C_t against the Log of hippocampal cDNA dilution showed a linear range with correlation coefficients ranging from 0.930 to 0.992. We later used these standard curves to interpolate the amount of amplified PKB, PKC δ , CAK β , PTP ζ/β , and 18S cDNA from CA1, CA3, and dentate gyrus of Naïve, Pseudotrained, and spatially Trained rats. The target amount was divided by the endogenous reference (18S rRNA) amount to obtain a normalized target expression value.

3. Results

3.1. Acquisition of spatial discrimination

In the present studies, we used a cDNA microarray approach to profile changes in gene expression within

the hippocampus during spatial information processing. We specifically studied gene expression in spatial discrimination learning with the holeboard food search task, designed and implemented as a task in which animals discriminate between relevant (baited) and irrelevant (not baited) holes (Oades & Isaacson, 1978). As such, it is a land-based spatial learning task that can be used to record both reference and working memory measures (Oades, 1981, van der Zee, Compaan, de Boer, & Luiten, 1992; Vázquez et al., 2000). As opposed to the more commonly used Morris water maze, in which animals are forced to swim in opaque water until they find an escape platform (Morris, Garrud, Rawlins, & O'Keefe, 1982), the holeboard food search task relies on a more ethological behavior for rodents: food searching. Like the Morris water maze, the holeboard food search task is sensitive to hippocampal lesions (Oades, 1981) and has been used to study various aspects of learning and memory (Isaacson, Yoder, & Varner, 1994; Maldonado-Irizarry & Kelley, 1995; van der Staay, van Nies, & Raaijmakers, 1990; van der Staay, 1999; van der Zee et al., 1992). Our previous studies showed increased hippocampal mRNA levels of the immediate-early transcription factor gene *hgf-3/nurr1*, which unfortunately is not represented on the arrays used here, 3 h after training on Day 3 of acquisition of this task (Peña de Ortiz et al., 2000). In addition, increased translocation of hippocampal calcium/phospholipid-dependent

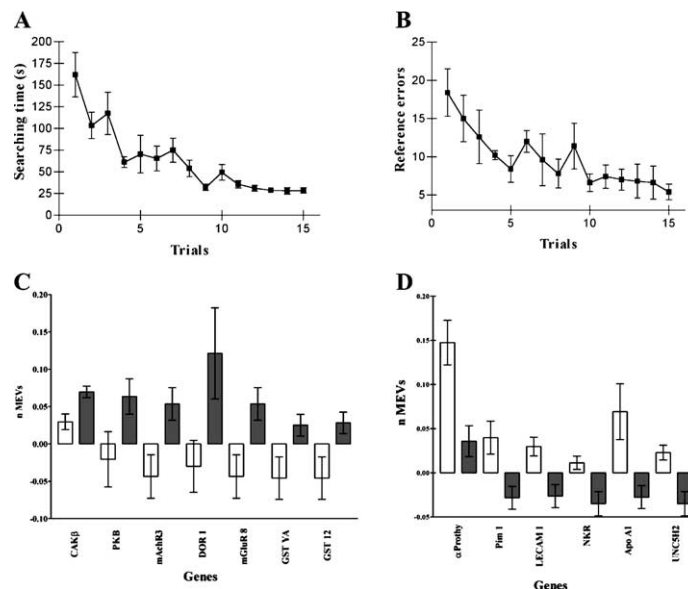


Fig. 1. Results of spatial training and microarray analysis. Graphs show the development of spatial discrimination learning in rats ($N = 12$). Means (\pm SEM) were calculated for a total of 12 rats from the Trained group. Spatial acquisition is shown by the significant decreases in the total searching time ($***p < .0001$) in the maze (A) and the number of reference errors, ($***p < .0001$; B), as well as in working errors ($***p < .001$, not shown). (C) Selected genes showing up regulation in the Trained (dark bars) versus the Naïve (white bars) conditions included cell adhesion kinase β (CAK β), protein kinase B (PKB), muscarinic acetylcholine receptor subtype 3 (mAChR3), δ opioid receptor 1 (DOR1), metabotropic glutamate receptor subtype 8 (mGluR8), and glutathione *S*-transferase YA and 12 (GST YA and GST 12). (E) Selected downregulated genes showing higher expression in the Naïve (white bars) versus the Trained (dark bars) conditions included prothymosin α (α Prothy), Pim 1 serine/threonine kinase (Pim 1), L-selectin precursor 1 (LECAM1), natural killer lymphocyte receptor (NKR), apolipoprotein A1 (APO A1), and a netrin receptor (UNC5H2).

protein kinase C (PKC) was also observed at this particular time point of acquisition of the same task (Vázquez et al., 2000). Thus, we chose to use the Day 3, 3 h time point to determine what other changes in gene expression could be occurring in the hippocampus as a result of spatial training and acquisition.

Rats in the trained group displayed spatial learning as shown by a significant decrease in searching time ($***p < .0001$, Fig. 1A) and in the number of reference errors ($***p < .0001$, Fig. 1B) as determined by one-way ANOVA. The number of working errors ($***p < .0005$) was also significantly reduced (data not shown). Post hoc analysis found significant differences in searching time for trials 4–15 compared to trial 1 ($**p < .001$), for trials 12–15 compared to trial 2 ($*p < .05$), and for trials 12–15 compared to trial 3 ($**p < .001$). Likewise, post hoc analysis of the reference errors found significant differences for trials 12–15 compared to trials 1 ($***p < .0001$) and 2 ($*p < .05$ for the comparison with

trials 12 and 13; $**p < .001$ for the comparison with trials 14 and 15). Reference errors for trials 13–15 were also significantly reduced compared to trial 3 ($*p < .05$).

3.2. Analysis of gene expression

To establish a hippocampal gene expression profile we trained rats in a holeboard spatial discrimination task for three consecutive days and performed expression analysis using cDNA microarrays. A total of 19 genes showed significant differences in expression, representing approximately 3% of the total number of genes examined. Table 1 lists the genes showing significant changes in hippocampal expression based on our microarray analysis. The list includes genes encoding proteins related to various aspects of neurotransmission, signal transduction, and intracellular kinase networks. None of the housekeeping genes on the array showed

Table 1
Genes showing regulated expression after spatial training

Gene description	Accession Number	Expression change
<i>Axonal growth and guidance</i>		
Transmembrane receptor UNC5H2	U87306	▼*
Apolipoprotein A-1 (APO-AI)	M00001	▼*
<i>Signal transduction</i>		
M-ras protein	D89863	▲*
<i>Neurotransmitter and neuropeptide receptors</i>		
Muscarinic acetylcholine receptor M3	M18088	▲*
Glutamate metabotropic receptor 8	U63288	▲*
D(2) dopamine receptor	M36831	▲*
Delta-type-opioid receptor	U00475	▲*
<i>Protein kinase and phosphatase networks</i>		
Pim-1 serine/threonine kinase	X63675	▼*
Protein kinase Cδ	M18330	▼*
c-akt proto-oncogene, protein kinase B	D30040	▲*
Receptor protein-tyrosine phosphatase ζ/β	U09357	▲*
Cell adhesion kinase β (CAK β)	D45854	▲*
<i>Nuclear proteins</i>		
Prothymosin α	M20035 M86564	▼*
<i>Lymphocyte receptors and cell surface antigens</i>		
NK lymphocyte receptor	U56936	▼**
L-selectin precursor (LEG AM 1)	D10831	▼*
<i>Oxidative stress</i>		
Glutathione S-transferase YA subunit (GST-YA)	K01931	▲*
Glutathione S-transferase microsomal (GST 12, MGST1)	J03752	▲*
<i>General metabolism</i>		
Liver carboxylesterase 10 precursor (ES-10)	L46791	▼*
Glucagon receptor precursor (GL-R)	L04796	▼*

Genes that showed statistically significant (*, **) changes in expression with either methods of normalization (HK and ALL). Genes are organized by their general function as it may relate to synaptic plasticity. The GenBank Accession Numbers are depicted, as well as the kind of expression change observed (up-regulation, ▲; down-regulation, ▼). The genes marked with † were identified by normalization against the expression of housekeeping genes, while those marked with ‡ were identified based on normalization of the microarray data against the mean signal of all the genes on the array. Unmarked genes were selected based on normalization by both methods.

significant changes in expression. Of the 19 significant genes, 10 (marked with †) were selected based on normalization by housekeeping gene expression, 2 (marked by ‡) were selected based on normalization by the signal of all the genes on the array, and 7 (unmarked) were selected by using both normalization methods.

Fig. 1C shows several of the upregulated genes including neuroreceptors known for their modulatory effects on neurotransmission such as those encoding DOR1, ($*p < .05$), the metabotropic glutamate receptor 8 (mGluR 8, $*p < .05$), and the muscarinic acetylcholine receptor subtype 3 (mAChR3, $*p < .05$). Signaling molecules in the protein kinase and phosphatase category included CAK_{β} ($*p < .05$) and PKB ($*p < .05$), which were up regulated after training. Finally, genes encoding antioxidative proteins, such as glutathione *S*-transferases (GST-YA, $*p < .05$ and GST 12, $*p < .05$) were up regulated after spatial training. On the other hand, the hippocampal expression of the genes encoding PKC δ ($*p < .05$) and Pim-1 serine/threonine kinase ($*p < .05$) were down regulated after spatial training (Fig. 1D). Other down-regulated genes included those encoding proteins involved in lipid transfer to regenerating axons such as apolipoprotein A-1 (APO A-1, $*p < .05$), netrin receptors related to regeneration, migration and axonal guidance (Shifman & Selzer, 2000; Stuermer & Bastmeyer, 2000) such as UNC5H2 ($*p < .05$ $*p < .05$), and proteins related to immunity defense such as the genes encoding the nuclear factor prothymosin α (α Prothy, $*p < .05$), the cell surface antigen L-selectin precursor 1 (LECAM1, $**p < .005$), and the natural killer lymphocyte receptor (NKR, $**p < .01$) (Fig. 1D).

3.3. Molecular validation studies

For confirmation of the gene expression changes observed by our microarray analysis we focused on several of our candidate genes identified by statistical analysis of our microarray data and used additional Naïve and Trained animals. We used Northern blot analysis to test the hippocampal expression of *prothymosin α* mRNA, which encodes a highly acidic nuclear protein that seems to play an important role in the immune system (Baxevanis et al., 1992; Shiau, Chen, Liao, Huang, & Wu, 2001) and could play a role in gene regulation in the brain. As shown in Fig. 2A, the results confirmed that the levels of *prothymosin α* mRNA in the hippocampus are reduced after training in the spatial maze (Student's *t* test: $*p = .0248$), as was determined previously by our microarray approach (see Fig. 1D). We also verified the expression of the gene encoding DOR1, for which our microarray analysis determined a significant increase in mRNA levels after spatial training (Fig. 1C). Fig. 2B shows representative autoradiograms of in situ hybridization of coronal brain sections from Naïve and Trained rats. The results showed a modest, but significant,

training-related increase in hippocampal mRNA levels. Interestingly, the training-related changes in *dor1* mRNA levels seemed to be occurring mostly in the CA3 hippocampal subregion. Densitometric analysis of the whole hippocampal in situ hybridization signal confirmed the significant training-related increase in *dor1* mRNA (Student's *t* test: $***p = .001$, Fig. 2C). Moreover, one-way ANOVA of Northern blot data (Fig. 2D) revealed significant differences in hippocampal *dor1* mRNA levels between Naïve, Pseudotrained (see below), and spatially-Trained rats ($*p = .0138$). Post-testing analysis showed that both Pseudotrained and spatially Trained rats had higher hippocampal *dor1* mRNA levels than Naïve controls ($*p < .05$ each comparison). No difference was observed between the spatially Trained rats and the Pseudotrained controls ($p > .05$). Thus, the hippocampal changes in *dor1* mRNA seen after spatial discrimination learning are probably related to general maze experience rather than to development of a spatial-associative map of food location within the maze. It is important to note, however, that the changes observed in the Pseudotrained controls showed higher variability than the other two groups (Barlett's test: $**p = .0088$). Thus, changes in hippocampal *dor1* mRNA levels related to general maze experience seem to show significantly higher individual variability than changes related to spatial learning. Fig. 2E shows typical patterns of hole visits for Pseudotrained and spatially Trained rats. Unlike Trained rats, the Pseudotrained controls did not learn a specific spatial map of food location, but rather visited holes randomly throughout training. Thus, Pseudotrained animals did not develop spatial preferences for specific holes.

We also considered it important to verify that genes not showing statistically significant changes with the microarray approach showed similar results when utilizing an alternative technique for evaluating gene expression. For this purpose, we focused on the *cadherin K* gene, which was not determined to change ($p > .1$) in our experiment based on the analysis of the microarray data, and which is a member of the cadherin family of cell adhesion proteins thought to play important roles at the synapse (Fannon & Colman, 1996; Inoue, Tanaka, Suzuki, & Takeichi, 1998). Densitometric analysis of in situ hybridizations of coronal brain sections from Naïve and Trained animals (not shown) confirmed that no significant change in the mean expression of *cadherin K* mRNA occurred in the hippocampus ($p = .5934$), whereas a significant increase in *cadherin K* mRNA occurred in the cortex as a result of spatial training ($*p = .0471$).

3.4. Validation by LCM and real time PCR

So far, we had confirmed the training related expression changes of 2 genes. However, an important question remaining was whether the changes detected in

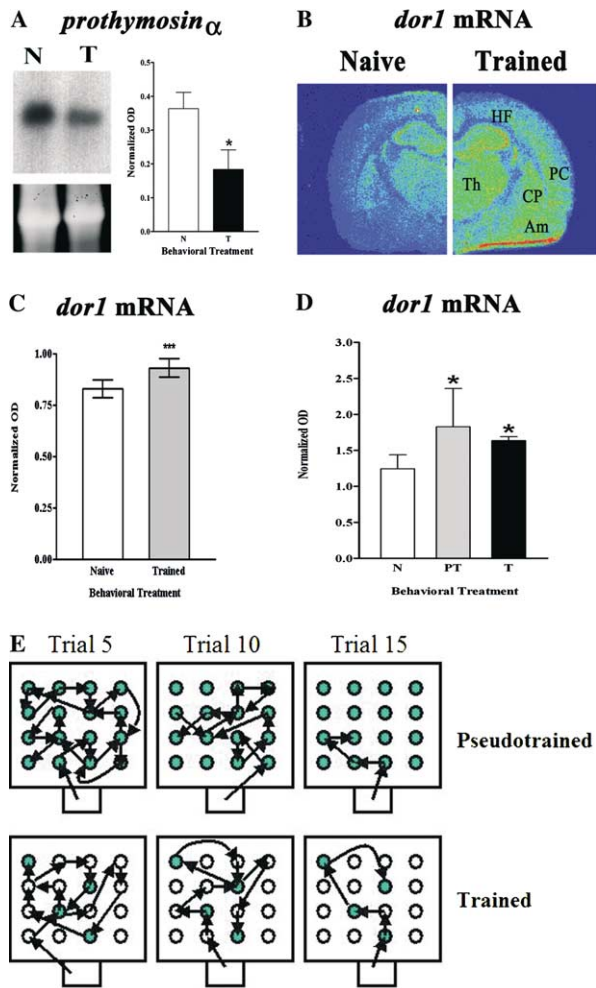


Fig. 2. Regulation of *prothymosin α* and *dor1* mRNA as a result of spatial training. (A) Spatial training related downregulation of *prothymosin α* was verified using Northern blotting. The left panel shows representative autoradiographic data and staining of ribosomal bands (bottom). The left panel shows a bar graph depicting the results of densitometry analysis of *prothymosin α* mRNA in the hippocampus, indicating that this gene is significantly downregulated as a result of spatial training (black bar; $*p < .05$) compared to Naïve controls (white bars). The Northern analysis was repeated three times, each time with total RNA extracted from pooled hippocampi obtained from 3 animals per group. Thus, while the total number of animals used was 9, the N for the Northern blot data is 3. (B) Representative autoradiograms from Naïve and Trained animals showing increased hippocampal levels of *dor1* mRNA 3 h after spatial discrimination learning on Day 3. Pseudocolor scheme for expression levels: magenta < blue < green < yellow < red. (C) Densitometry analysis showing significant hippocampal upregulation of *dor1* mRNA as measured by *in situ* hybridization ($***p < .005$; $N = 5$) Trained rats (grey bars) compared to Naïve controls (white bars). (D) Densitometry analysis showing significant hippocampal up regulation of *dor1* mRNA in Naïve (white bars), Pseudotrained (grey bars), and spatially Trained (black bars) rats, as measured by Northern blotting ($**p = .005$). Post-testing determined that both Pseudotrained and Trained rats displayed higher hippocampal *dor1* mRNA levels than Naïve controls. (E) Representative pattern of food searching in Pseudotrained and Trained rats at Trials 5, 10, and 15 of acquisition. Colored circles represent baited holes in the maze.

the microarray study corresponded to spatial learning-specific processes or just general maze experience. Thus, a pseudotrained-yoked control was used (Fig. 2E), in addition to the Naïve and Trained animals. Animals in the new group experienced yoked pseudotraining, which consisted in exploring and consuming food pellets in a fully baited maze (no spatial food pattern) during sessions that lasted the same amount of time as the time used by the spatially trained partner or after having consumed all the food pellets in the maze. For these additional studies we focused on differentially expressed genes, such as PKC δ (O'Driscoll, Teng, Fabbro, Greene, & Weinstein, 1995), PKB (Lin et al., 2001), and RPTP ζ/β (Coussens, Williams, Ireland, & Abraham, 2000; Uetani et al., 2000), involved in signaling cascades associated to long-term potentiation (LTP) and other plasticity-related hippocampal events. We selected these three genes together with CAK β , a cell adhesion kinase also related to LTP (Ali & Salter, 2001; Huang et al., 2001), for validation using real-time PCR of RNA extracted from hippocampal cells procured with LCM. These techniques allowed us to detect changes in gene expression within specific hippocampal structures. Fig. 3 is an example from the dentate gyrus region before (A) and after (B) granule cells were extracted by LCM. Cells were also obtained from CA1 and CA3 regions (data not shown). The procured cells attached to the cap (Fig. 3C) were used to isolate total RNA, from which cDNA was synthesized and used to perform standard RT-PCR and real time PCR (see below). Fig. 3D shows that a single product of the expected size for glyceraldehyde-3-phosphate dehydrogenase (GAPDH) was obtained from RT-PCR of CA1 (not shown), CA3 (lane 2) and dentate gyrus (lane 4) cDNA. The lack of products in the mock reactions (lanes 3 and 5) indicates that the obtained amplification products did not originate from contaminating genomic DNA.

We next used the non-specific DNA-intercalator, SYBR green I, to perform real-time PCR. Amplification plots and melting temperature analysis for the four genes studied were generated using whole hippocampal cDNA as a template to assess the efficiency of real-time PCR and to rule-out the possibility of generating unwanted PCR products or primer-dimers, respectively (Bustin, 2000). Fig. 4 shows typical amplification plots obtained for 18S rRNA (A) and RPTP ζ/β (B). Background-subtracted relative fluorescence units (RFU) were plotted against the cycle number to determine the threshold cycle or C_t , which is defined as the amplification cycle in which significant fluorescence signal is first detected. Similar curves were obtained in different experiments and with the other three genes studied (data not shown). The increase in C_t with the progressive dilution of hippocampal cDNA demonstrated the sensitivity of the method. Amplification plots of each of the four genes and of 18S rRNA were used to generate

standard curves from which expression levels of experimental samples were interpolated (see below). The increases in RFU corresponded to a single product as was

observed in the melting temperature curve analysis of the amplified products (Figs. 4C and D), which takes advantage of the fact that the fluorescence of the inter-

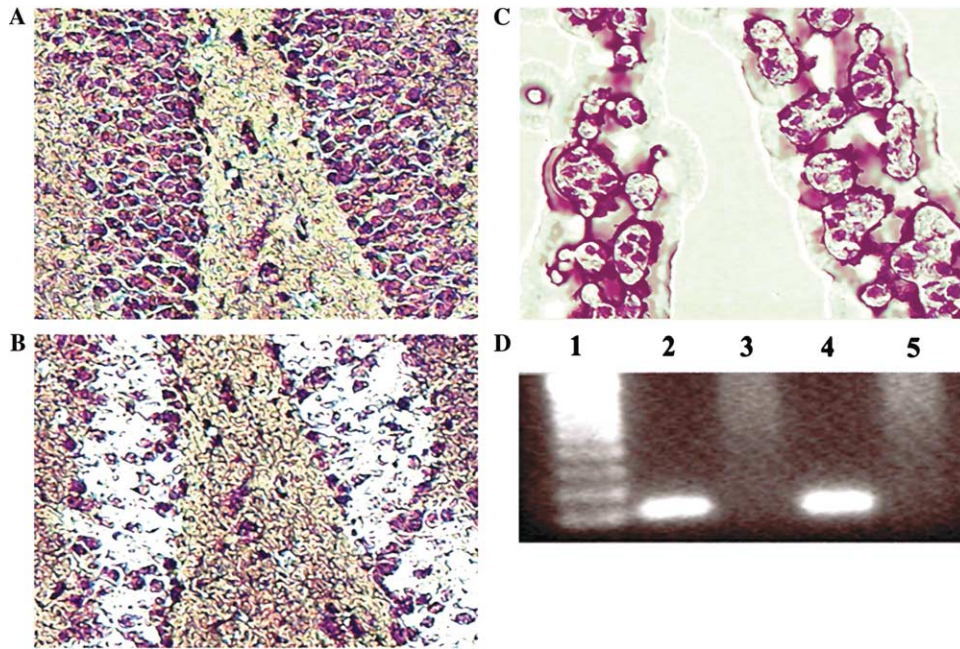
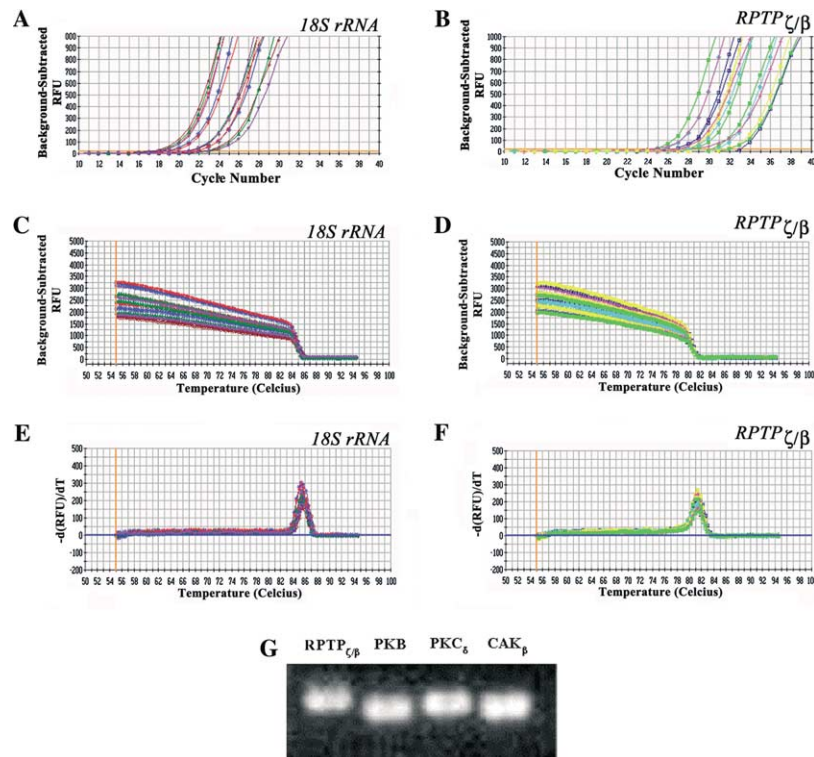


Fig. 3. LCM from Nissl-stained sections. Coronal brain sections were stained with thionin and dehydrated just before capture. (A) Granule cells of the dentate gyrus before capture. (B) Dentate gyrus area after captures. (C) Captured dentate gyrus granule cells. (D) Results of RT-PCR performed on RNA extracted from captured cells using GAPDH primers. Lane 1, 50 Kb DNA ladder; lane 2, amplified product from CA3 procured cells; lane 3, mock reaction showing no non-specific amplification product; lane 4, amplified product from dentate gyrus procured cells; and lane 5, mock reaction.



calated dye decreases as the amplified products are denatured. As seen in both graphs, the serial dilutions of hippocampal cDNA all resulted in products of the same melting temperature value, 85 °C for the 18S rRNA product (Fig. 4C), and 81 °C for the RPTP $_{\zeta/\beta}$ product (Fig. 4D). The unique peaks at 85 and 81 °C in the first derivative plots for 18S rRNA and RPTP $_{\zeta/\beta}$, respectively, which were calculated based on the melting temperature curve analysis of the same real-time PCR products obtained in Figs. 4C and D, also indicated that each of the reactions yielded only one amplification product. Finally, a 2% agarose gel electrophoresis analysis further confirmed the specificity of the primers and the presence of just one RT-PCR product for RPTP $_{\zeta/\beta}$ (188 bp), PKB (116 bp), PKC $_{\delta}$ (122 bp), and CAK $_{\beta}$ (100 bp, Fig. 4G).

Fig. 5 shows the results of the quantitative real-time PCR studies on cDNA prepared from the cell layers of the CA1, CA3, and dentate gyrus subregions of the hippocampus of Naïve, Pseudotrained, or spatially Trained rats. PKB expression in spatially trained animals resulted in significant up regulation of the gene in distinct hippocampal regions (Fig. 5A), a result that confirmed the findings obtained with our microarray analysis. As shown in Fig. 5A, one-way ANOVA for each region confirmed the up regulation of PKB mRNA in CA1 (* $p = .0268$). Multiple comparisons testing with the Newman–Keuls post-test showed a specific difference only between the Pseudotrained and Trained conditions (* $p < .05$). On the other hand, no significant changes in PKB mRNA expression occurred in the CA3 region as a result of neither training nor pseudotraining. For the dentate gyrus, while the observed changes in PKB mRNA expression follow a similar pattern of that observed in CA1, the changes did not reach statistical significance ($p = .0763$), probably because of the high variability in the Naïve and Trained groups. Student's t tests did not identify differences between the groups either.

CAK $_{\beta}$ is an extracellular matrix adhesion protein that resulted in up regulation in the microarray studies (Fig. 1C). As seen in Fig. 5B, one-way ANOVA of the changes in CAK $_{\beta}$ mRNA expression in CA1 and CA3 showed a down regulation of gene expression in these regions,

(**** $p = .0001$). Post-testing showed specific significant differences between the three groups (** $p < .001$ for each comparison). Interestingly, the granule cells of the dentate gyrus showed a 3-fold up regulation in spatially trained animals when compared to Naïve and Pseudotrained controls. While a one-way ANOVA did not identify a significant difference between the groups for the dentate gyrus expression data, a Student's t test comparing Naïve and Trained animals confirmed the statistically significant up regulation of CAK $_{\beta}$ mRNA in this hippocampal subregion (** $p = .0086$).

Fig. 5C shows our results with RPTP $_{\zeta/\delta}$, which also confirmed the findings obtained from the microarray analysis. Importantly, this gene was one of the two genes found to be significant only with the ALL normalization method (see Table 1). While no significant effect by the behavioral treatments was observed for CA1, the CA3 subregion showed a significant difference between the groups when tested by one-way ANOVA (* $p = .0473$), although the higher expression levels in the Trained condition did not reach statistical significance when compared to the Naïve and Pseudotrained controls in the post-hoc tests. Nevertheless, a striking 5-fold up-regulation was observed on RPTP $_{\zeta/\delta}$ mRNA levels in the dentate gyrus (**** $p < .0001$) as determined by one-way ANOVA. Multiple comparisons post-testing showed a significant difference between the Trained group and both the Naïve (** $p < .001$) and Pseudotrained conditions ($p < .001$), but not between these two control groups.

Finally, PKC $_{\delta}$ was one of the genes showing down-regulated expression in the microarray studies using whole hippocampi. LCM coupled to real-time PCR revealed that such down regulation is due mainly to an effect on the granule cells of the dentate gyrus (Fig. 5D). Specifically, for CA1 the results of one-way ANOVA showed a non-significant down regulation of PKC $_{\delta}$ mRNA levels ($p = .0662$). In contrast, PKC $_{\delta}$ mRNA in the CA3 hippocampal subregion showed a small, but significant up regulation (* $p = .0067$). Specific comparisons between Trained and Naïve or Trained and Pseudotrained showed significant differences between the groups (** $p < .01$ and * $p < .05$, respectively). Interestingly, the basal levels of PKC $_{\delta}$ mRNA in the dentate



Fig. 4. Results from optimized real-time PCR for 18S rRNA and RPTP $_{\zeta/\beta}$ using the SYBR green I dye method. cDNA from rat hippocampus was serially diluted and real-time PCR was performed as described in the methods section. Each dilution is represented by a different color in each plot. (A)–(B) Representative real-time PCR amplification curves of 18S rRNA and RPTP $_{\zeta/\beta}$ for a set of dilutions of cDNA from rat hippocampus. Background-subtracted RFU values were calculated for cycles 10–40 by subtracting the baseline RFU obtained in cycles 2–10. The RFU threshold level in which signal is higher than background is indicated in both cases with the horizontal orange line. (C)–(D) After the real-time PCR was completed, a melting temperature curve analysis of the amplification product was performed, which determined that the reaction yielded only one product and was free of DNA contaminants or primer–dimers. (E)–(F) The presence of one peak when we plotted the first derivative of the RFU values [–d(RFU)], obtained in the melting analysis, as a function of temperature also demonstrated that just one product was present. (G) Results from a representative 2% agarose gel electrophoresis of RT-PCR products for each of the four genes studied confirmed that the peak observed in the first derivative plots corresponded to a single band of the size predicted to each of the four genes.

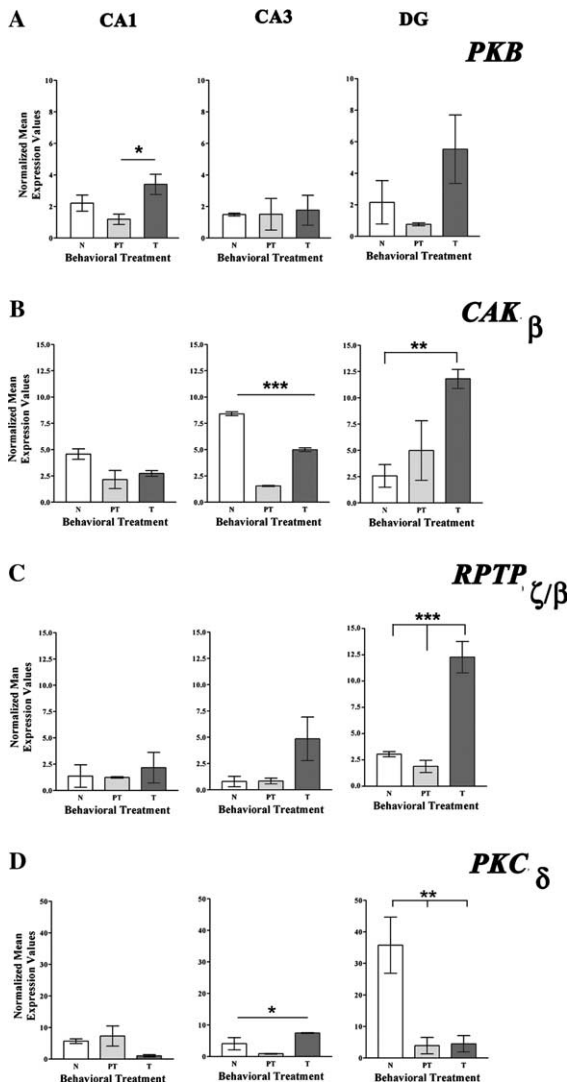


Fig. 5. Differential expression of selected candidate genes among hippocampal subregions in association to maze experience or spatial learning. Bar graphs showing differences in gene expression between LCM procured CA1, CA3, and dentate gyrus (DG) cells of Naïve (N), Pseudotrained (PT) and spatially Trained (T) animals ($N = 3$) as determined by quantitative real-time PCR. Reactions were done in triplicate. The graphs depict the normalized mean expression values and the SEM for each condition and hippocampal region. (A) Spatial learning specific increases in PKB gene expression in CA1 ($*p < .05$) and DG ($p > .05$) cells, respectively. No changes in PKB expression occurred in CA3 pyramidal cells. (B) Significant down regulation of CAK β expression in pseudotrained ($***p < .001$) and spatially trained ($***p < .001$) animals, compared to Naïve animals, in the CA3 subregion. A 3-fold increase in expression in Trained vs Naïve animals occurred in the dentate gyrus subregion ($**p < .01$). (C) Spatial learning specific increases in RPTP ζ/β expression in the CA3 ($p > .05$) and dentate gyrus regions ($***p < .001$ for each comparison). (D) A small up regulation of PKC δ in the CA3 region ($**p < .01$ for N vs T; $*p < .05$ for PT vs T) and a dramatic down regulation in the dentate gyrus ($**p < .01$ for each comparison).

gyrus of Naïve animals are 7-fold higher, when compared to the levels in the pyramidal cell layers. Moreover, both Pseudotraining and Training caused a

dramatic decrease in PKC δ mRNA levels when compared to the Naïve control (one-way ANOVA, $p = .0038$). Post-testing confirmed the significant down-regulation of PKC δ mRNA in the Pseudotrained ($**p < .01$) and the Trained groups ($**p < .01$), when compared to Naïve controls. No difference was found between Pseudotrained and Trained animals, suggesting that the change in expression was due to the general maze experience and not specifically to spatial discrimination learning.

4. Discussion

By applying the cDNA microarray approach we have been able to define a gene expression profile in a particular brain region, the hippocampus; at a particular time during a learning and memory consolidation process, 3 h after the end of training on Day 3 of acquisition of the holeboard food search task. The statistical tests utilized in our studies allowed us to select a relatively small number of candidate genes on the arrays, which can be more carefully studied as to their role in learning and memory. In our study, we found increased expression of the mRNAs encoding DOR1, mGLUR8, and mAChR3, indicating that opioidergic, glutaminergic, and cholinergic transmission is modulated in the hippocampus as a result of spatial training. One interesting possibility is that increased expression of DOR1 and mGLUR8 is related to neurotransmission at hippocampal mossy fiber-CA3 synapses, which have been shown to display opioid receptor dependent-LTP (Derrick, Rodríguez, Lieberman, & Martinez, 1992) and glutaminergic transmission involving metabotropic receptors (Chen, Huang, & Hsu, 2001; Tzounopoulos, Janz, Sudhof, Nicoll, & Malenka, 1998). Cholinergic synapses, which have been shown to be important in learning (Browne, Lin, Mattsson, Georgievska, & Isacson, 2001; Motooka et al., 2001; Rauch & Raskin, 1984), modulate excitatory transmission directly in associational-commissural synapses in CA3 and indirectly in the mossy fiber synapses by increasing GABA release (Vogt & Regehr, 2001). Similarly, a network of intracellular kinases and phosphatases is thought to be essential for the processing of information in the brain (Roberson et al., 1999; Sweatt, 2001a, 2001b). Accordingly, we found that the expression of the genes encoding PKB, PKC δ , and CAK β , among others (see below), was modulated in the hippocampus after spatial training.

When performing statistical analysis of roughly 600 genes simultaneously with an established significance threshold of $*p < .05$, one could expect that approximately 5% (i.e., 30) of the genes tested could indeed be false positive. In fact, this has been a topic of large discussion in the microarray field, which is still unresolved (Newton, Kendziorski, Richmond, Blattner, &

Tsui, 2001; Tseng, Oh, Rohlin, Liao, & Wong, 2001). Some have suggested the utilization of more conservative p values (i.e., .001) when comparing two conditions, which has the disadvantage of possibly being too restrictive, thereby resulting in the misclassification of true positives (Benjamini, Drai, Elmer, Kafkafi, & Golani, 2001; Hochberg & Benjamini, 1990; Keselman, Cribbie, & Holland, 2002). We believe, based on the results of our molecular validation tests, which confirmed 6 of the 19 significant genes, that the strategy used here shows that standard statistical tests can be applied to microarray data using p values of $<.05$ as the hallmark for classifying a gene as significant. Such significant genes may be considered validated as to their change in expression in the tissues and conditions used for the microarray studies. Indeed, whole tissue gene profiling may misrepresent the level of change of a gene within a particular brain structure because different effects could be occurring in different cell populations, as evidence by our LCM studies.

Our results also demonstrate that training in a spatial task can result in hippocampal changes in gene expression that may be subregion specific, as well as related to either general maze experience or specific spatial learning processes, or both. Pseudotrained controls have been used by others when studying the specificity of cellular changes related to acquisition of the holeboard spatial discrimination task used here (van der Zee et al., 1992). In our studies, the Pseudotrained control animals were also “yoked” or paired to a spatially Trained partner. First, both Pseudotrained and Trained animals spent approximately the same amount of time in the maze, thus general exploration of the context was avoided in both groups. Second, as the Trained animals acquired the task and spent less time in each trial, the yoked Pseudotrained partners were consequently removed before they could consume all the food pellets. For the Pseudotrained rats, the amount of time and food consumed varied throughout the trials, depending on the learning rate of their yoked Trained partners. Since all the holes were baited throughout all the trials for the Pseudotrained rats, these animals did not need to develop a spatial-associative map of food location in the maze. Furthermore, our observation that Pseudotrained rats visited the holes randomly confirms that they did not develop associative spatial discrimination. However, other forms of non-associative contextual learning probably do occur.

In our gene profiling with real-time PCR, PKB, a serine-threonine protein kinase also known as Akt, showed spatial learning-specific up regulation only in the dentate gyrus and CA1 subregions, suggesting that its induction could be related to *N*-methyl-D-aspartate (NMDA) receptor signaling similar and perhaps to LTP in these areas (Grosshans, Clayton, Coultrap, & Browning, 2002; Nicoll & Malenka, 1999; Richter-Le-

vin, Canevari, & Bliss, 1995). In fact, our results are in agreement with findings showing increased phosphorylation of PKB by the phosphatidylinositol 3-kinase (PI-3 kinase) in CA1 protein extracts prepared after induction of NMDA receptor-dependent LTP in the Schaffer collateral/commissural-CA1 pathways (Sanna et al., 2002). PI-3 kinase activation of PKB has also been shown to be mediated via NMDA receptor activation in striatal neurons (Perkinton, Ip, Wood, Crossthwaite, & Williams, 2002). CAK_{β} is a focal adhesion kinase that activates Src and thereby up regulates NMDA receptor function (Huang et al., 2001). Interestingly, our results showed a significant down regulation of CAK_{β} mRNA levels in area CA3, which does not display NMDA receptor-dependent LTP (Derrick et al., 1992; Do, Martinez, Martinez, & Derrick, 2002; Grover & Yan, 1999), but a 3-fold increase in expression compared to the Naïve condition in the granule cells of the dentate gyrus (Fig. 7B), which do display NMDA receptor-dependent LTP (Hoh, Beiko, Boon, Weiss, & Cain, 1999; Lee & Kesner, 2002; Min, Asztely, Kokaia, & Kullmann, 1998). These changes seemed to also occur to a lesser degree in the pseudotrained animals, suggesting that the expression of this gene might be influenced not only by spatial learning processes, but also by general exploratory behavior in the maze.

On the other hand, $RPTP_{\zeta/\beta}$, a member of the receptor protein tyrosine phosphatase superfamily, showed a spatial learning specific 3-fold induction in its mRNA levels in the granule cells of the dentate gyrus. Interestingly, $RPTP$ family members are comparable to tyrosine receptor kinases or TRKs and have been shown to respond to a variety of proteic ligands. Specifically, $RPTP_{\zeta/\beta}$'s apparent ligand is a member of the immunoglobulin-like neuronal cell adhesion molecules known as contactin or F3 (Thomaidou et al., 2001). Both $RPTP_{\zeta/\beta}$ and contactin are neuron-specific proteins expressed in several brain regions including the hippocampus (Cho et al., 1998; Hosoya et al., 1995; Kawachi, Fujikawa, Maeda, & Noda, 2001; Virgintino et al., 1999). They have both been suggested to be important in establishing important neural contacts during development and synaptic plasticity (Holland, Peles, Pawson, & Shlessinger, 1998; Maeda & Noda, 1998; Murai, Misner, & Ranscht, 2002). However, a study using mice lacking $RPTP_{\zeta/\beta}$ did not find any neurodevelopmental abnormalities in such animals, suggesting that the function of $RPTP_{\zeta/\beta}$ is not essential during development (Harroch et al., 2000). It would be interesting, however, based on our present findings to examine the capacities of adult $RPTP_{\zeta/\beta}$ mouse mutants in hippocampal dependent learning and memory tasks and LTP. In support of this idea, studies using mice lacking $RPTP_{\delta}$ showed that receptor phosphatase signaling in the hippocampus is relevant to both spatial learning and LTP (Uetani et al., 2000).

Finally, for PKC δ , a member of the calcium-independent/phospholipid-dependent novel PKC isotypes, basal level of mRNA expression in the granule cells suffered a significant down-regulation as a result of maze training. On the other hand, a modest, yet significant, spatial learning-specific increase in expression occurred in area CA3. Interestingly, a previous study reported decreased protein levels of PKC δ in the dentate gyrus granule cell layer and increased PKC δ levels in the hippocampal pyramidal cell layers 24 h after treatment with the glutamate structural analogue, kainic acid (McNamara, Wees, & Lenox, 1999). Thus, it will be interesting to determine the role of NMDA receptors on PKC δ mRNA down regulation following maze experience.

The approach used in our study has allowed us to obtain a *molecular snapshot* of the cellular events related to learning in the hippocampus at a specific moment in the acquisition/consolidation process. Overall, our findings confirmed our predictions based on the synaptic plasticity hypothesis in that learning involves changes in the expression of proteins related to neurotransmission, cell signaling, cell–cell communication, and also changes in genes encoding nuclear proteins. In addition, the present studies establish a data extraction, normalization, and statistical analysis approach applied to nylon membrane microarrays and radioactive probes, which are available to most molecular biology laboratories and can be used as a screening method to identify candidate genes modulated in selected brain regions by behavioral experience. The identified genes can be considered as candidates for functional validation studies assessing the effects of temporal and regional restriction of their expression on behavioral plasticity and memory.

Acknowledgments

We thank Dr. Alcino J. Silva for his helpful comments on this manuscript. This work was supported by NIH (S.P.O. Grants NIGMS-MBRS SOGGMO 8102-26S1 and NINDS-SNRP U54 NS39405; U.P.R. Grant NCCR-RCMI 2G12RRO3641) and MRISP Grant MH 48190.

References

- Adams, M. D., Kerlavage, A. R., Fields, C., & Venter, J. C. (1993). 3400 New expressed sequence tags identify diversity of transcripts in human brain. *Nature Genetics*, *4*, 256–267.
- Albright, T. D., Kandel, E. R., & Posner, M. I. (2000). Cognitive neuroscience. *Current Opinion in Neurobiology*, *10*, 612–624.
- Ali, D. W., & Salter, M. W. (2001). NMDA receptor regulation by Src kinase signalling in excitatory synaptic transmission and plasticity. *Current Opinion in Neurobiology*, *11*, 336–342.
- Alvarez, P., Zola-Morgan, S., & Squire, L. R. (1994). The animal model of human amnesia: Long-term memory impaired and short-term memory intact. *Proceedings of National Academy of Sciences USA*, *91*, 5637–5641.
- Bailey, C. H., Bartsch, D., & Kandel, E. R. (1996). Toward a molecular definition of long-term memory storage. *Proceedings of National Academy of Sciences USA*, *93*, 13445–13452.
- Baxevanis, C. N., Thanos, D., Reclos, G. J., Anastasopoulos, E., Tsokos, G. C., Papamatheakis, J., & Papamichail, M. (1992). Prothymosin alpha enhances human and murine MHC class II surface antigen expression and messenger RNA accumulation. *Journal of Immunology*, *148*, 1979–1984.
- Benjamini, Y., Drai, D., Elmer, G., Kafkafi, N., & Golani, I. (2001). Controlling the false discovery rate in behavior genetics research. *Behavioural Brain Research*, *125*, 279–284.
- Bonaventure, P., Guo, H., Tian, B., Liu, X., Bittner, A., Roland, B., Salunga, R., Ma, X. J., Kamme, F., Meurers, B., Bakker, M., Jurzak, M., Leysen, J. E., & Erlander, M. G. (2002). Nuclei and subnuclei gene expression profiling in mammalian brain. *Brain Research*, *943*, 38–47.
- Browne, S. E., Lin, L., Mattsson, A., Georgievska, B., & Isacson, O. (2001). Selective antibody-induced cholinergic cell and synapse loss produce sustained hippocampal and cortical hypometabolism with correlated cognitive deficits. *Experimental Neurology*, *170*, 36–47.
- Bustin, S. A. (2000). Absolute quantification of mRNA using real-time reverse transcription polymerase chain reaction assays. *Journal of Molecular Endocrinology*, *25*, 169–193.
- Castellucci, V. F., Blumenfeld, H., Golet, P., & Kandel, E. R. (1989). Inhibitor of protein synthesis blocks long-term behavioral sensitization in the isolated gill-withdrawal reflex of *Aplysia*. *Journal of Neurobiology*, *20*, 1–9.
- Chen, Y. L., Huang, C. C., & Hsu, K. S. (2001). Time-dependent reversal of long-term potentiation by low-frequency stimulation at the hippocampal mossy fiber-CA3 synapses. *Journal of Neuroscience*, *21*, 3705–3714.
- Cho, H., Shimazaki, K., Takeuchi, K., Kobayashi, S., Watanabe, K., Oguro, K., Masuzawa, T., & Kawai, N. (1998). Biphasic changes in F3/contactin expression in the gerbil hippocampus after transient ischemia. *Experimental Brain Research*, *122*, 227–234.
- Coussens, C. M., Williams, J. M., Ireland, D. R., & Abraham, W. C. (2000). Tyrosine phosphorylation-dependent inhibition of hippocampal synaptic plasticity. *Neuropharmacology*, *39*, 2267–2277.
- Derrick, B. E., Rodríguez, S. B., Lieberman, D. N., & Martinez, J. L., Jr. (1992). Mu opioid receptors are associated with the induction of hippocampal mossy fiber long-term potentiation. *Journal of Pharmacology and Experimental Therapeutics*, *263*, 725–733.
- Do, V. H., Martinez, C. O., Martinez, J. L., Jr., & Derrick, B. E. (2002). Long-term potentiation in direct perforant path projections to the hippocampal CA3 region in vivo. *Journal of Neurophysiology*, *87*, 669–678.
- Fannon, A. M., & Colman, D. R. (1996). A model for central synaptic junctional complex formation based on the differential adhesive specificities of the cadherins. *Neuron*, *17*, 423–434.
- Flexner, L. B., Flexnor, J. B., & Stellar, E. (1965). Memory and cerebral protein synthesis in mice as affected by graded amounts of puromycin. *Experimental Neurology*, *13*, 254–272.
- Frey, U., Krug, M., Reymann, K. G., & Matthies, H. (1988). Anisomycin, an inhibitor of protein synthesis blocks late phases of LTP phenomena in the hippocampal CA1 region in vitro. *Brain Research*, *452*, 57–65.
- Geschwind, D. H. (2000). Mice, microarrays, and the genetic diversity of the brain. *Proceedings of National Academy of Sciences USA*, *20*, 10676–10678.
- Gonzalez, G. A., & Montminy, M. R. (1989). Cyclic AMP stimulates somatostatin gene transcription by phosphorylation of CREB at serine 133. *Cell*, *59*, 675–680.

- Grosshans, D. R., Clayton, D. A., Coultrap, S. J., & Browning, M. D. (2002). LTP leads to rapid surface expression of NMDA but not AMPA receptors in adult rat CA1. *Nature Neuroscience*, 5, 27–33.
- Grover, L. M., & Yan, C. (1999). Evidence for involvement of group II/III metabotropic glutamate receptors in NMDA receptor-independent long-term potentiation in area CA1 of rat hippocampus. *Journal of Neurophysiology*, 82, 2956–2969.
- Gudi, T., Casteel, D. E., Vinson, C., Boss, G. R., & Pilz, R. B. (2000). NO activation of fos promoter elements requires nuclear translocation of G-kinase I and CREB phosphorylation but is independent of MAP kinase activation. *Oncogene*, 19, 6324–6333.
- Harroch, S., Palmeri, M., Rosenbluth, J., Custer, A., Okigaki, M., Shrager, R., Blum, M., Buxbaum, J. D., & Schlessinger, J. (2000). No obvious abnormality in mice deficient in receptor protein tyrosine phosphatase β . *Molecular and Cellular Biology*, 20, 7706–7715.
- Hochberg, Y., & Benjamini, Y. (1990). More powerful procedures for multiple significance testing. *Statistics of Medicine*, 9, 811–818.
- Hoh, T., Beiko, J., Boon, F., Weiss, S., & Cain, D. P. (1999). Complex behavioral strategy and reversal learning in the water maze without NMDA receptor-dependent long-term potentiation. *Journal of Neuroscience*, 19, RC2.
- Holland, S. J., Peles, E., Pawson, T., & Shlessinger, J. (1998). Cell-contact-dependent signaling in axon growth and guidance: Eph receptor tyrosine kinases and receptor protein tyrosine phosphatase β . *Current Opinion in Neurobiology*, 8, 117–127.
- Hosoya, H., Shimazaki, K., Kobayashi, S., Takahashi, H., Shirasawa, T., Takenawa, T., & Watanabe, K. (1995). Developmental expression of the neural adhesion molecule F3 in the rat brain. *Neuroscience Letters*, 186, 83–86.
- Huang, Y., Lu, W., Ali, D. W., Pelkey, K. A., Pitcher, G. M., Lu, Y. M., Aoto, H., Roder, J. C., Sasaki, T., Salter, M. W., & MacDonald, J. F. (2001). CAK β /Pyk2 kinase is a signaling link for induction of long-term potentiation in CA1 hippocampus. *Neuron*, 29, 485–496.
- Inoue, T., Tanaka, T., Suzuki, S. C., & Takeichi, M. (1998). Cadherin-6 in the developing mouse brain: Expression along restricted connection systems and synaptic localization suggest a potential role in neuronal circuitry. *Developmental Dynamics*, 211, 338–351.
- Isaacson, R. L., Yoder, P. E., & Varner, J. (1994). The effects of pregnenolone on acquisition and retention of a food search task. *Behavioural and Neural Biology*, 61, 170–176.
- Ithaka, R., & Gentleman, R. R. (1996). A language for data analysis and graphics. *Journal of Computational and Graphical Statistics*, 5, 299–314.
- Kandel, E. R., Castellucci, V. F., Goelet, P., & Schacher, S. (1987). Cell-biological interrelationships between short-term and long-term memory. *Research Publications—Association for Research in Nervous and Mental Disorder*, 65, 111–132.
- Kawachi, H., Fujikawa, A., Maeda, N., & Noda, M. (2001). Identification of GIT1/Cat-1 as a substrate molecule of protein tyrosine phosphatase ζ/β by the yeast substrate-trapping system. *Proceedings of National Academy of Sciences USA*, 98, 6593–6598.
- Keselman, H. J., Cribbie, R., & Holland, B. (2002). Controlling the rate of Type I error over a large set of statistical tests. *British Journal of Mathematical and Statistical Psychology*, 55, 27–39.
- Kessner, R. P., & Connor, S. (1972). Independence of short-term memory: A neuronal system analysis. *Science*, 176, 432–434.
- Lee, I., & Kesner, R. P. (2002). Differential contribution of NMDA receptors in hippocampal subregions to spatial working memory. *Nature Neuroscience*, 5, 162–168.
- Lee, M. T., Kuo, F. C., Whitmore, G. A., & Sklar, J. (2000a). Importance of replication in microarray gene expression studies: Statistical methods and evidence from repetitive cDNA hybridizations. *Proceedings of National Academy of Sciences USA*, 97, 9834–9839.
- Lee, C. K., Weindruch, R., & Prolla, T. A. (2000b). Gene-expression profile of the ageing brain in mice. *Nature Genetics*, 25, 294–297.
- Lin, C. H., Yeh, S. H., Lin, C. H., Lu, K. T., Leu, T. H., Chang, W. C., & Gean, P. W. (2001). A role for the PI-3 kinase signaling pathway in fear conditioning and synaptic plasticity in the amygdala. *Neuron*, 31, 841–851.
- Liew, C. C., Hwang, D. M., Fung, Y. W., Laurensen, C., Cukerman, E., Tsui, S., & Lee, C. Y. (1994). A catalogue of genes in the cardiovascular system as identified by expressed sequence tags. *Proceedings of National Academy of Sciences USA*, 91, 10645–10649.
- Maeda, N., & Noda, M. (1998). Involvement of receptor-like protein tyrosine phosphatase ζ /RPTP β and its ligand pleiotrophin/heparin-binding growth-associated molecule (HB-GAM) in neuronal migration. *Journal of Cell Biology*, 142, 203–216.
- Maldonado-Irizarry, C. S., & Kelley, A. E. (1995). Excitotoxic lesions of the core and shell subregions of the nucleus accumbens differentially disrupt body weight regulation and motor activity in rat. *Brain Research Bulletin*, 38, 551–559.
- Matynia, A., Anagnostaras, S. G., & Silva, A. J. (2001). Weaving the molecular and cognitive strands of memory. *Neuron*, 32, 557–559.
- Mayr, B., & Montminy, M. (2001). Transcriptional regulation by phosphorylation-dependent factor CREB. *Natural Reviews Molecular Cell Biology*, 2, 599–609.
- McNamara, R. K., Wees, E. A., & Lenox, R. H. (1999). Differential subcellular redistribution of protein kinase C isozymes in the rat hippocampus induced by kainic acid. *Journal of Neurochemistry*, 72, 1735–1743.
- Min, M. Y., Asztely, F., Kokaia, M., & Kullmann, D. M. (1998). Long-term potentiation and dual-component quantal signaling in the dentate gyrus. *Proceedings of National Academy of Sciences USA*, 95, 4702–4707.
- Montarolo, P. G., Goelet, P., Castellucci, V. F., Morgan, J., Kandel, E. R., & Schacher, S. (1986). A critical period for macromolecular synthesis in long-term heterosynaptic facilitation in Aplysia. *Science*, 234, 1249–1254.
- Morris, R. G., Garrud, P., Rawlins, J. N., & O'Keefe, J. (1982). Place navigation impaired in rats with hippocampal lesions. *Nature*, 297, 681–683.
- Motooka, Y., Kondoh, T., Nomura, T., Tamaki, N., Tozaki, H., Kanno, T., & Nishizaki, T. (2001). Selective cholinergic denervation inhibits expression of long-term potentiation in the adult but not infant rat hippocampus. *Brain Research Development and Brain Research*, 129, 119–123.
- Murai, K. K., Misner, D., & Ranscht, B. (2002). Contactin supports synaptic plasticity associated with hippocampal long-term depression but not potentiation. *Current Biology*, 12, 181–190.
- Nicoll, R. A., & Malenka, R. C. (1999). Expression mechanisms underlying NMDA receptor-dependent long-term potentiation. *Annals of New York Academy of Sciences*, 868, 515–525.
- Nisenbaum, L. K. (2002). The ultimate chip shot: Can microarray technology deliver for neuroscience? *Genes, Brain and Behavior*, 1, 27–34.
- Newton, M. A., Kendzierski, C. M., Richmond, C. S., Blattner, F. R., & Tsui, K. W. (2001). On differential variability of expression ratios: Improving statistical inference about gene expression changes from microarray data. *Journal of Computational Biology*, 8, 37–52.
- Oades, R. D. (1981). Impairments of search behaviour in rats after haloperidol treatment, hippocampal or neocortical damage suggest a mesocorticolimbic role in cognition. *Biological Psychology*, 12, 77–85.
- Oades, R. D., & Isaacson, R. L. (1978). The development of food search behavior by rats: The effects of hippocampal damage and haloperidol. *Behavioural Biology*, 24, 327–337.
- O'Driscoll, K. R., Teng, K. K., Fabbro, D., Greene, L. A., & Weinstein, I. B. (1995). Selective translocation of protein kinase C-

- δ in PC12 cells during nerve growth factor-induced neuriteogenesis. *Molecular Biology of the Cell*, 6, 449–458.
- Peña de Ortiz, S., Maldonado-Vlaar, C. S., & Carrasquillo, Y. (2000). Hippocampal expression of the orphan nuclear receptor gene *hzf-3/nurr1* during spatial discrimination learning. *Neurobiology of Learning and Memory*, 74, 161–178.
- Perkinton, M. S., Ip, J. K., Wood, G. L., Crossthwaite, A. J., & Williams, R. J. (2002). Phosphatidylinositol 3-kinase is a central mediator of NMDA receptor signalling to MAP kinase (Erk1/2), Akt/PKB and CREB in striatal neurones. *Journal of Neurochemistry*, 80, 239–254.
- Rauch, S. L., & Raskin, L. A. (1984). Cholinergic mediation of spatial memory in the preweanling rat: Application of the radial arm maze paradigm. *Behavioural Neuroscience*, 98, 35–43.
- Richter-Levin, G., Canevari, L., & Bliss, T. V. (1995). Long-term potentiation and glutamate release in the dentate gyrus: Links to spatial learning. *Behavioural Brain Research*, 66, 37–40.
- Roberson, E. D., English, J. D., Adams, J. P., Selcher, J. C., Kondratieck, C., & Sweatt, J. D. (1999). The mitogen-activated protein kinase cascade couples PKA and PKC to cAMP response element binding protein phosphorylation in area CA1 of hippocampus. *Journal of Neuroscience*, 19, 4337–4348.
- Sanna, P. P., Cammalleri, M., Berton, F., Simpson, C., Lutjens, R., Bloom, F. E., & Francesconi, W. (2002). Phosphatidylinositol 3-kinase is required for the expression but not for the induction or the maintenance of long-term potentiation in the hippocampal CA1 region. *Journal of Neuroscience*, 22, 3359–3365.
- Shiau, A. L., Chen, Y. L., Liao, C. Y., Huang, Y. S., & Wu, C. L. (2001). Prothymosin alpha enhances protective immune responses induced by oral DNA vaccination against pseudorabies delivered by *Salmonella choleraesuis*. *Vaccine*, 19, 3947–3956.
- Shifman, M. I., & Selzer, M. E. (2000). Expression of netrin receptor UNC-5 in lamprey brain: Modulation by spinal chord transection. *Neurorehabilitation and Neural Repair*, 14, 49–58.
- Stuermer, C. A., & Bastmeyer, M. (2000). The retinal axon's pathfinding to the optic disk. *Progress in Neurobiology*, 62, 197–214.
- Sweatt, J. D. (2001a). The neuronal MAP kinase cascade: A biochemical signal integration system subserving synaptic plasticity and memory. *Journal of Neurochemistry*, 76, 1–10.
- Sweatt, J. D. (2001b). Protooncogenes subserve memory formation in the adult CNS. *Neuron*, 31, 671–674.
- Thomaidou, D., Coquillat, D., Meintanis, S., Noda, M., Rougon, G., & Matsas, R. (2001). Soluble forms of NCAM and F3 neuronal cell adhesion molecules promote Schwann cell migration: Identification of protein tyrosine phosphatases ζ/β as the putative F3 receptors on Schwann cells. *Journal of Neurochemistry*, 78, 767–778.
- Tseng, G. C., Oh, M. K., Rohlin, L., Liao, J. C., & Wong, W. H. (2001). Issues in cDNA microarray analysis: Quality filtering, channel normalization, models of variations and assessment of gene effects. *Nucleic Acids Research*, 29, 2549–2557.
- Tsien, J. Z. (2000). Linking Hebb's coincidence-detection to memory formation. *Current Opinion in Neurobiology*, 10, 266–273.
- Tzounopoulos, T., Janz, R., Sudhof, T. C., Nicoll, R. A., & Malenka, R. C. (1998). A role for cAMP in long-term depression at hippocampal mossy fiber synapses. *Neuron*, 21, 837–845.
- Uetani, N., Kato, K., Ogura, H., Mizuno, K., Kawano, K., Mikoshiba, K., Yakura, H., Asano, M., & Iwakura, Y. (2000). Impaired learning with enhanced hippocampal long-term potentiation in PTP δ -deficient mice. *EMBO Journal*, 19, 2775–2785.
- van der Staay, F. J., van Nies, J., & Raaijmakers, W. (1990). The effects of aging in rats on working and reference memory performance in a spatial holeboard discrimination task. *Behavioural and Neural Biology*, 53, 356–370.
- van der Staay, F. J. (1999). Spatial working memory and reference memory of Brown Norway and WAG rats in a holeboard discrimination task. *Neurobiology of Learning and Memory*, 71, 113–125.
- van der Zee, E. A., Compaan, J. C., de Boer, M., & Luiten, P. G. (1992). Changes in PKC gamma immunoreactivity in mouse hippocampus induced by spatial discrimination learning. *Journal of Neuroscience*, 12, 4808–4815.
- Vázquez, S. I., Vázquez, A., & Peña de Ortiz, S. (2000). Different hippocampal activity profiles for PKA and PKC in spatial discrimination learning. *Behavioural Neuroscience*, 114, 1109–1118.
- Virgintino, D., Ambrosi, M., Errico, P., Bertossi, M., Papadaki, C., Karageos, D., & Gennarini, G. (1999). Regional distribution and cell type-specific expression of the mouse F3 axonal glycoprotein: A developmental study. *Comparative Neurology*, 413, 357–372.
- Vogt, K. E., & Regehr, W. G. (2001). Cholinergic modulation of excitatory synaptic transmission in the CA3 area of the hippocampus. *Journal of Neuroscience*, 21, 75–83.